Reversible Hydration Enabling High-Rate Aqueous Li-ion Batteries

Leiting Zhang, Franziska Kühling, Agnes-Matilda Mattsson, Xu Hou, Gustav Ek, Thomas Dufils, Chao Zhang, William R. Brant, Kristina Edström, Erik J. Berg*

Department of Chemistry – Ångström Laboratory, Uppsala University, Box 538, SE 751 21 Uppsala, Sweden.

Corresponding Author

*Leiting Zhang, leiting.zhang@kemi.uu.se.

ABSTRACT

Two-dimensional TiS_2 has been proposed as a versatile host material for various battery chemistries. Nevertheless, its compatibility with aqueous electrolytes has not been thoroughly understood. Herein, we report on a reversible hydration process to account for the electrochemical activity and structural evolution of TiS_2 in a dilute electrolyte for sustainable aqueous Li-ion batteries. Solvated water molecules intercalate into TiS_2 layers together with Li^+ cations, forming a hydrated phase with a nominal formula unit of $Li_{0.38}(H_2O)_{2-\delta}TiS_2$ as the end-product. We unambiguously confirm the presence of two layers of intercalated water by complementary electrochemical cycling, *operando* structural characterization, and computational simulation. Such a process is fast and reversible, delivering 60 mAh g^{-1} discharge capacity at a current density of 1250 mA g^{-1}. Our work provides further design principles for high-rate aqueous Li-ion batteries based on reversible water co-intercalation.

TOC GRAPHICS

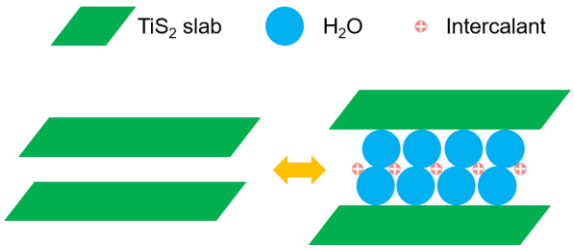

While batteries for electric vehicles have been dominated by Li-ion technology, alternative chemistries are regaining unprecedented attentions to account for society's colossal need for grid energy storage. By replacing toxic and flammable organic electrolyte solvents with water, the cost can be lowered and safety further enhanced.[1] However, the 1.23 V electrochemical stability window (ESW) of water significantly impedes the development of modern aqueous batteries. In this context, various thermodynamic and kinetic strategies have been proposed to widen the electrolyte ESW.[2–11]

Recently, we reported cycling TiS_2 in a dilute aqueous electrolyte containing 2 m (molality, mol kg^{-1}) of LiTFSI.[12] By online electrochemical mass spectrometry coupled with three-electrode cycling, we ascribed the electrochemical reactivity to combined intercalation, water electrolysis, and partial TiS_2 exfoliation. Yet, the exact intercalation mechanism remained unclear. In particular, the TiS_2 electrode cycled in aqueous electrolytes possessed a peculiar potential profile, upshifted from that cycled in non-aqueous electrolytes by ca. 500 mV. Such a difference cannot be simply explained by the different activity of Li^+ in the 2 m electrolyte.

Among various possibilities, water co-intercalation appears to be the most plausible explanation. It is widely acknowledged that solvent co-intercalation into TiS_2 may take place in non-aqueous Li-ion and Na-ion batteries.[13–15] However, aqueous batteries powered by water intercalating into TiS_2 has not yet been investigated to our knowledge, apart from the early work by Whittingham[16] and Schöllhorn[17,18] in the 1970s on the hydrated phases of A_xTiS_2 (A = alkali metal). Owing to the low electrode potential, moisture sensitivity[16] and electrocatalytic activity[19] of TiS_2, attention of the research community was rapidly switched to layered oxides,[20] which led to the birth of modern Li-ion batteries.

In this work, we revisit the classic TiS_2 electrode in aqueous Li-ion batteries *via* electrochemical cycling, in-house *operando* and synchrotron-based *in situ* X-ray diffraction (XRD), and molecular dynamics (MD) simulation. We unambiguously confirm a highly reversible TiS_2 hydration process as the main intercalation mechanism. Our findings provide timely insights into designing sustainable and high-rate aqueous batteries based on hydrated intercalants, in which the role of water should be critically assessed.

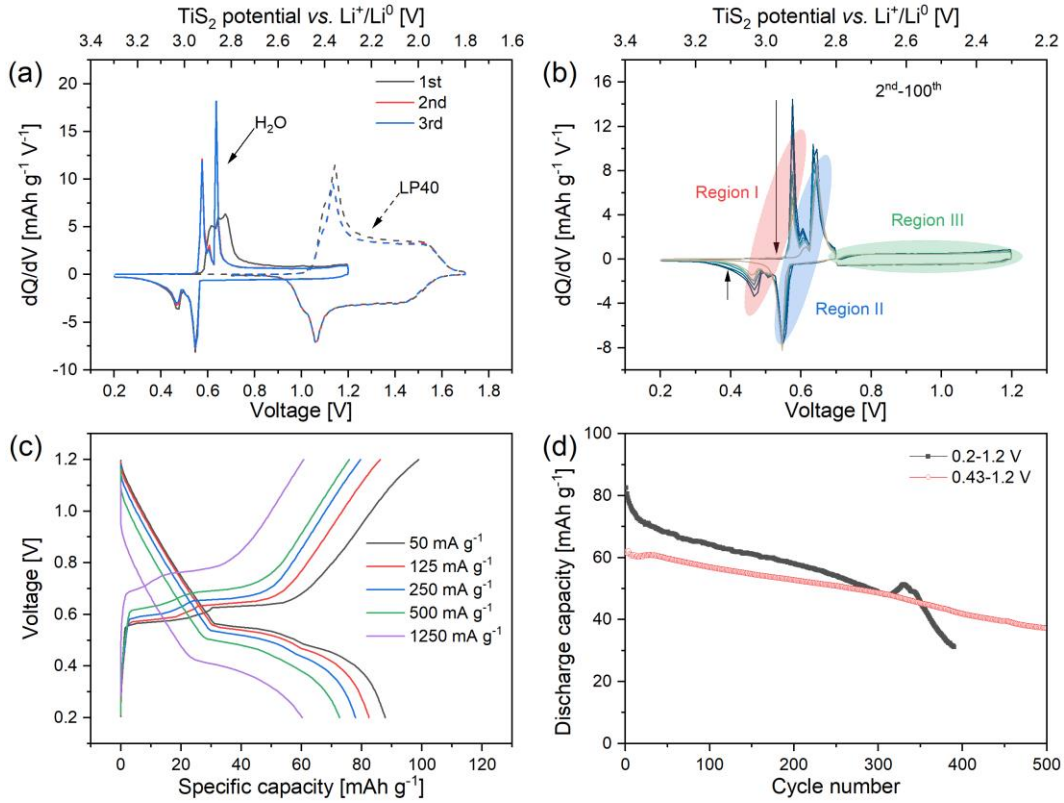

Figure 1. (a) dQ/dV curves of $LiFePO_4$ || TiS_2 cells cycled in aqueous and non-aqueous electrolytes. (b) dQ/dV curves of aqueous cells cycled between 0.2–0.7 V and 0.7–1.2 V of the first 100 cycles. Three regions are highlighted with distinct redox behaviors. (c) Rate capability of the aqueous cell. (f) Capacity retention of aqueous cells cycled at 250 mA g^{-1} with different voltage windows.

To evaluate the performance of TiS_2, $LiFePO_4$ (oversized) || TiS_2 cells were tested in both non-aqueous (1 mol L^{-1} of $LiPF_6$ in ethylene carbonate/diethyl carbonate (1:1), denoted as LP40) and aqueous electrolyte (2 m of LiTFSI in water). When cycled at 50 mA g^{-1}, the non-aqueous cell delivered a reversible capacity of ca. 203 mAh g^{-1}, while that of the aqueous cell was ca.

88 mAh g^{-1} (Figure S1 in the supporting information). The differential capacity (dQ/dV) curves of the non-aqueous cell in Figure 1(a) resemble those reported in the literature – a solid-solution–like redox couple centered around 2.25 V *vs.* Li^+/Li^0. In contrast, a distinct hump appears at ca. 2.85 V in the first charge of the aqueous cell. From the first discharge onwards, the cell possesses three regions of interest. The first two are around 2.97 V and 2.90 V, suggesting two sequential biphasic reactions. The third region spans between 2.80–2.30 V, showing a rectangular shape with solid-solution/capacitive behavior. Minor irreversibility is observed close to the end of charge, which is attributed to the hydrogen evolution reaction (HER).

To evaluate the co-existing biphasic and solid-solution behaviors of TiS_2, two aqueous cells were tested for 100 cycles within 0.2–0.7 V and 0.7–1.2 V voltage windows, respectively. The cycling curves are plotted in Figure S2 and their corresponding dQ/dV curves are compared in Figure 1(b). The dQ/dV curve of the low-voltage Region I is more asymmetric than the mid-voltage Region II. Upon extended cycling, performance degradation takes place first in Region I, then in Region II. Almost no capacity decay is observed in the high-voltage Region III.

The reaction kinetics of the three regions was also evaluated by rate capability tests. Specifically, aqueous cells were cycled under different current densities, ranging from 50 mA g^{-1} to 1250 mA g^{-1}. As shown in Figure 1(c), the cell delivered 60 mAh g^{-1} reversible discharge capacity in less than 3 min, corresponding to a nominal rate of 20C. It is also worth noting that most of the capacity decay is observed in Region I, while the slope of Region III remains largely unchanged.

Furthermore, extended cycling was performed at 250 mA g^{-1}. A reversible discharge capacity of 48.8 mAh g^{-1} was retained after 300 cycles, beyond which the capacity drastically faded (Figure 1(d)). When Region I was omitted from cycling (i.e. 0.43–1.2 V), 37.2 mAh g^{-1} discharge capacity

was retained after 500 cycles with a low capacity decay rate of ca. 0.1% per cycle, demonstrating the high reversibility of Regions II and III.

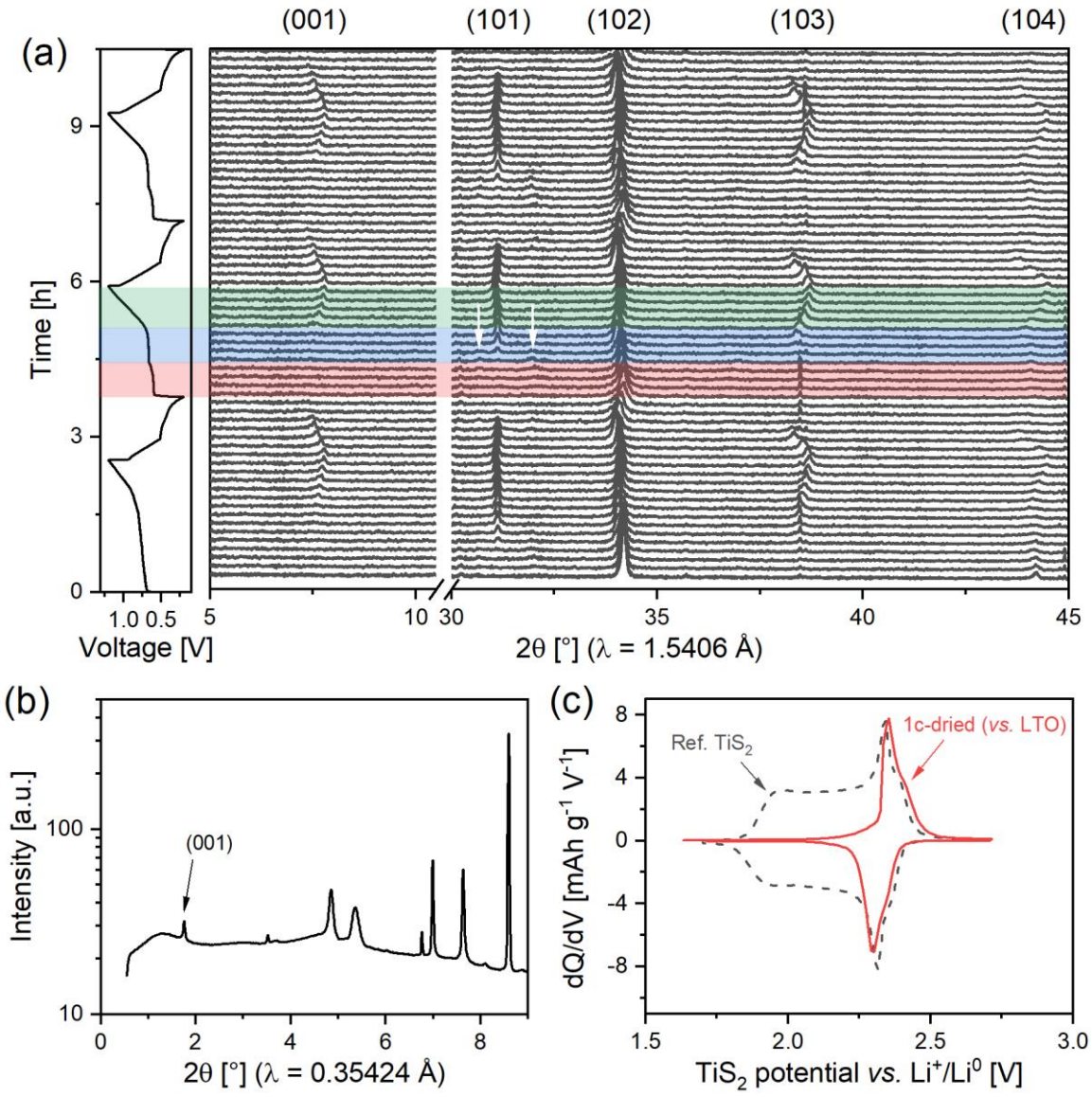

Figure 2. (a) In-house *operando* XRD of a $LiFePO_4$ || TiS_2 aqueous pouch cell. Regions I, II, and III are highlighted in the 2nd charge in red, blue, and green, respectively. White arrows highlight some unidentified peaks. (b) Synchrotron *in situ* XRD of a pouch cell stopped at the end of the charge. The (001) peak is highlighted with an arrow. (c) Comparison of dQ/dV curves between 1c-dried TiS_2 (solid line) and reference TiS_2 cycled in LP40 electrolyte (dash line).

Next, we investigated the dynamic structural change of TiS_2 by *operando* XRD. Measurements were conducted in transmission geometry using a Cu target and a pouch cell with a special holder

designed in-house.[21] Overall, reversible structural change is observed in Figure 2(a). Because of preferential orientation, the (001) peak of the pristine TiS_2 cannot be detected, which is a known issue reported elsewhere.[14] Also, strong absorption of the aqueous electrolyte and the stainless-steel current collector results in compromised data quality, therefore no conclusive remarks can be made towards Region I. A few extremely weak reflections around 30.6° and 32.0° can barely be observed from the XRD contour plots in Figure S3. Since they only appear in Region I, they are likely originating from an intermediate phase.

In Region II, several peaks at 7.5°, 31.0°, 34.2°, 38.7°, and 44.5° evolve, which are indexed to (001), (101), (102), (103), and (104) planes of the hexagonal unit cell of the intercalated phase, respectively. The interlayer spacing is estimated to be ca. 11.9 Å at the end of Region II (on charge), which is significantly larger than that of the pristine TiS_2 (5.7 Å). Since the van der Waals diameter of water amounts to ca. 3 Å,[22] two layers of water molecules would result in a lattice expansion of ca. 6 Å, which matches exceptionally well with the experimental result (11.9 Å – 5.7 Å = 6.2 Å).

In Region III, the (001) peak starts to drift to higher 2θ values, indicative of solid-solution reaction with a simultaneous compression in the *c*-direction. To get more accurate values, a cell stopped at the charged state was checked *in situ* by synchrotron XRD. The peak at 1.76° (2θ, when the X-ray wavelength λ = 0.35424 Å) in Figure 2(b) is assigned to the (001) reflection with an interlayer distance of 11.41 Å. The slight shrinkage can be explained by the reduced electrostatic repulsion of TiS_2 layers.

Next, we comment on what sets the reversible hydration of TiS_2 apart from electrodes containing structural water, such as vanadium oxide hydrates ($V_2O_5 \cdot nH_2O$). For example, the structural water is believed to effectively shield the charge density of Zn^{2+} and facilitate fast ion diffusion.[23–26] In

the case of dichalcogenide, the O–H···S interaction is much weaker.[16] To prove this, an aqueous cell was stopped at the charged state, the intercalated TiS_2 electrode was recovered and re-cycled in a non-aqueous full-cell after vacuum drying at 120 °C overnight (Figure 2(c) and Figure S4). The charged electrode, denoted as 1c-dried, delivered ca. 79 mAh g^{-1} capacity against a $Li_4Ti_5O_{12}$ (LTO) electrode in LP40 electrolyte, corresponding to 0.33 Li^+ release (based on its theoretical capacity of 238 mAh g^{-1}). The peak of the dQ/dV curve resembles that reported by Fleischmann and co-workers, who ascribed it to diffusion-limited lithiation of TiS_2.[27] It is therefore evident that intercalated water molecules have all been expelled by heating, while Li^+ ions remain in the restored TiS_2.

Molecular dynamics (MD) simulations were performed to provide more theoretical insight. The construction of the cell and simulation parameters are included in the supporting information. At open-circuit condition with an interlayer distance of 5.7 Å for the pristine TiS_2 (Figure 3(a)), no intercalation takes place. By increasing the interlayer distance and lowering the electrode potential, the kinetic barrier for Li^+ intercalation gets reduced and water also starts to intercalate, leading to Region I, where a monolayer of intercalated water molecules is observed in Figure 3(b–c). Here, Li^+ ions are found out of the plane formed by the oxygen atoms of the water molecules, while $TFSI^-$, owing to its size, is unable to enter the space between TiS_2 layers.

In Region II (Figure 3(d–e)), the intercalated water forms a bilayer, while Li^+ ions are found in the space between the two layers, with a very low probability within one of the layers. We also observe that this interlayer can accommodate $TFSI^-$ anions, with a ratio of ca. 1 $TFSI^-$ for 2 Li^+ ions. The lower intensity of the oxygen density peak compared to the monolayer case is explained by the presence of the $TFSI^-$ anions, owing to the large space it occupies between TiS_2 layers.

In Region III (Figure 3(f–g)), we still observe a bilayer of water with Li^+ intercalated in the space between the two layers, but with a narrower distribution. Contrary to Region II, $TFSI^-$ anions are almost completely absent, because of a higher accumulated charge and sufficiently low potential of the electrode.

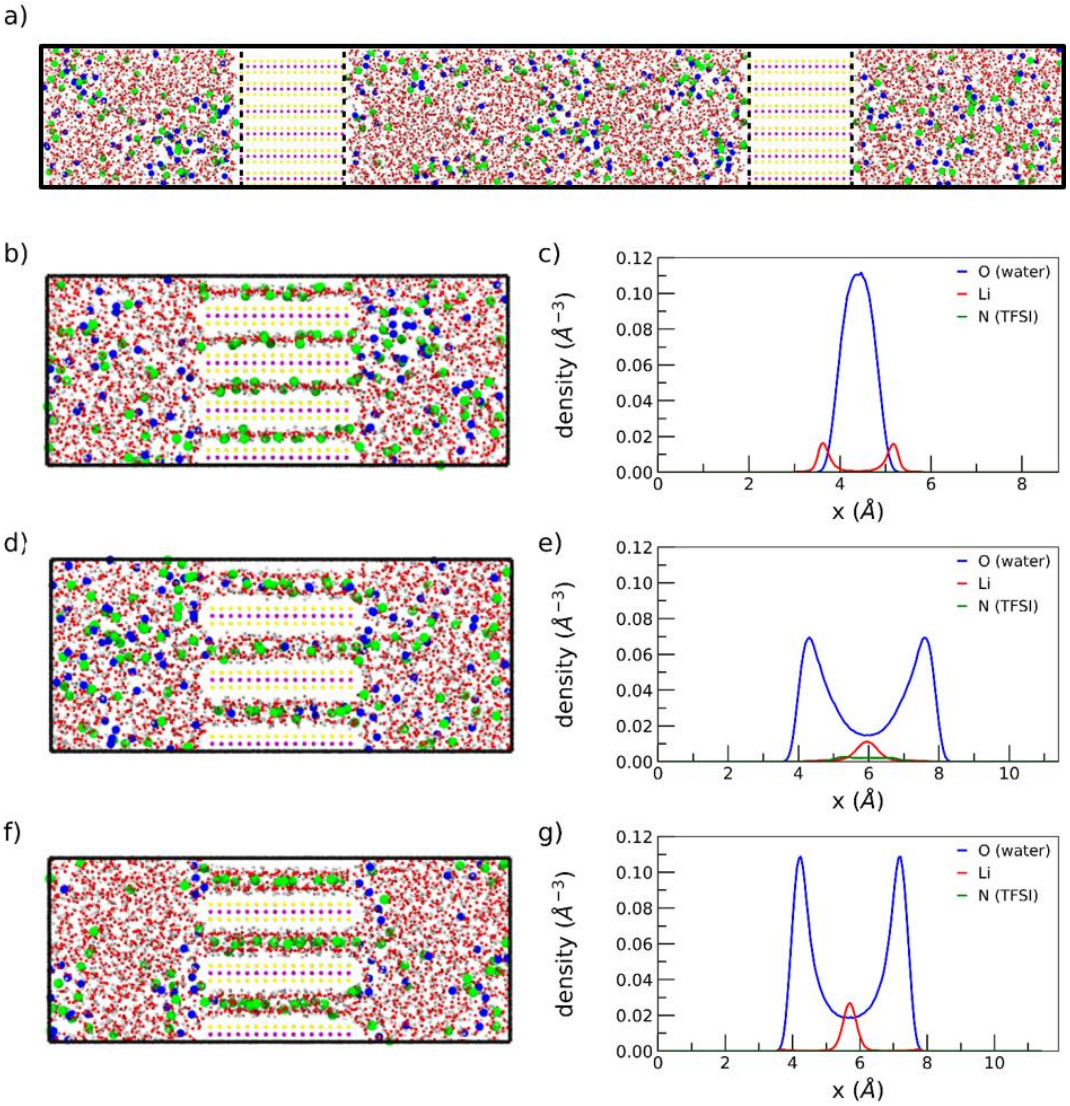

Figure 3. Snapshot of the MD simulation cell (a) for an interlayer distance of 5.7 Å at OCV, with oxygen (red), hydrogen (white), Ti (purple), S (yellow) and Li (green). For $TFSI^-$, only the N atom (blue) is shown. MD snapshots and atomic density profiles of the working electrode at 8.8 Å and –0.13 V vs. OCV (b–c), 11.9 Å and –0.19 V vs. OCV (d–e), 11.4 Å and –0.65 V vs. OCV (f–g), respectively. The density profiles are computed along the direction of the interlayer spacing and averaged over all the interlayers of the electrode. The origin is set at the position of the Ti plane.

Based on the complementary electrochemical testing, *operando* and *in situ* structural characterization, and computational simulation, we propose a comprehensive intercalation mechanism in Scheme 1 to account for the reversible electrochemical hydration of TiS_2 in aqueous electrolytes. Owing to the large hydration energy of Li^+ in aqueous solutions (–128 kcal mol^{-1}),[28] co-intercalation of hydrated Li^+ ions is thermodynamically favorable, resulting in an expansion of the interlayer distance. A monohydrate phase will form in Region I with a nominal composition of $Li_{0.13}(H_2O)_{1-\delta}TiS_2$, deduced from the specific capacity of the first redox plateau. The exact number of water molecules per TiS_2 is unknown, but it should be close to unity according to Whittingham.[16] The biphasic transition agrees with the plateau observed in Region I of Figure 1(b). Upon further intercalation, another layer of water can be accommodated by TiS_2, forming a dihydrate phase in Region II with a nominal composition of $Li_{0.25}(H_2O)_{2-\delta}TiS_2$. The biphasic transition results in another plateau observed in Region II of Figure 1(b). The hydrated Li^+ should be homogeneously distributed between TiS_2 layers, taking into account the electrically conducting nature of TiS_2, thus delocalized negative charges.[17] Since TiS_2 has been reported to accommodate at most two layers of water,[22] only Li^+ intercalation will take place in Region III. The gradual lithiation of the phase possesses a solid-solution behavior, which agrees with the sloping Region III of Figure 1(b) and the drifting (001) reflection in Figure 2(a). A nominal composition of the end-of-charge compound is deduced as $Li_{0.38}(H_2O)_{2-\delta}TiS_2$. Our value agrees well with that reported by Schöllhorn and Meyer, who showed that a lithium composition >0.4 would trigger hydrogen evolution.[18] On discharge, the reverse process takes place. Irreversibility is mainly observed in Region I, i.e. when removing all water from the monohydrate phase. A significant energy penalty is experienced, supported by the asymmetric dQ/dV curves of Region I in Figure 1(b).

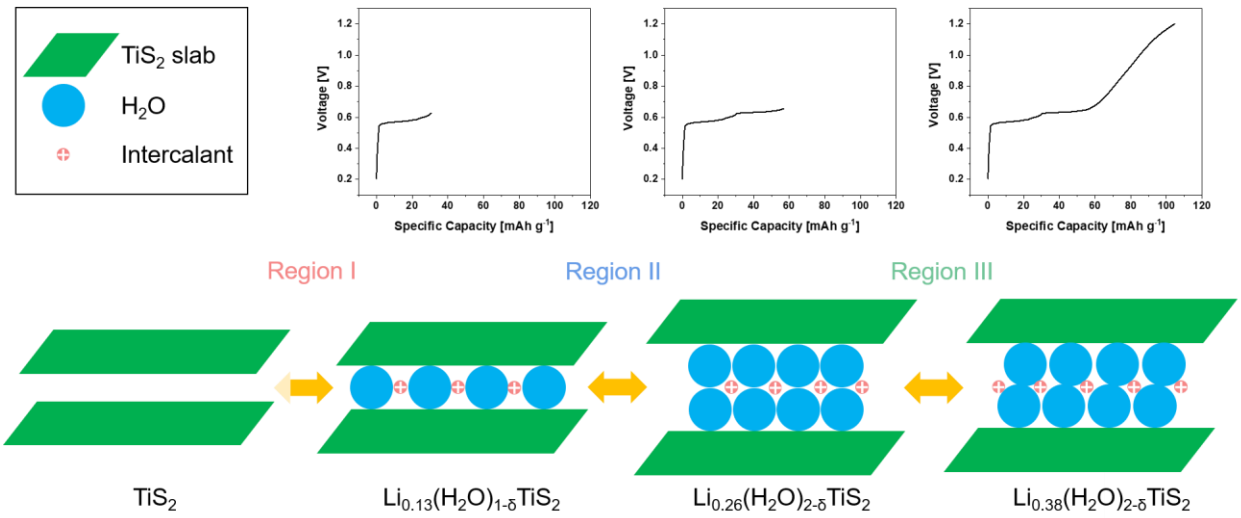

Scheme 1. Proposed reaction mechanism for reversible electrochemical hydration of TiS_2. Nominal compositions and structural evolutions are suggested for Regions I–III (not to scale).

There is a general consensus that an SEI is critical to prevent HER from happening for aqueous batteries, hence the need for either intrinsic or artificial SEI.[29] Recently, Droguet and co-workers have shown that inorganic artificial SEI is insufficient to prevent water reactivity for aqueous systems.[30] Elastic polymer grafting and film-forming additives are possible strategies to stabilize the anode–electrolyte interface. However, in a system like TiS_2, drastic lattice expansion and contraction take place in each cycle, imposing a serious challenge to the mechanical stability of the surface passivation layer. We have previously shown, by *operando* gas analysis, that no SEI is formed on TiS_2.[12] In fact, should there be a functioning SEI, hydrated Li^+ ions will have to dehydrate first, which would not result in water co-intercalation. Therefore, we believe that for electrodes following reversible hydration mechanism, an SEI is not a prerequisite. Consequently, the electrolyte ESW will be compromised, as in our case only ca. 0.4 Li^+ can be stored per TiS_2, beyond which water reduction will inevitably proceed. We are now screening possible electrolyte co-solvents, which could effectively alter the solvation structure of Li^+ and thus the redox behavior.

Lastly, the universality of the proposed mechanism remains to be verified in other aqueous systems, i.e. when Li^+ is replaced by larger cations, such as Na^+ and K^+, bearing in mind that the latter may have different hydration structures.[31] It would also be interesting to examine other 2D materials, such as MoS_2 and MXenes, which have also been proposed as intercalation electrodes for aqueous batteries.[32]

In summary, we report fundamental understanding of the electrochemical activity and structural evolution of TiS_2 in aqueous Li-ion batteries. We demonstrate a cooperative Li^+ and water co-intercalation process as the main intercalation mechanism. Up to two layers of water can be reversibly stored between TiS_2 layers. The resulting aqueous full-cell demonstrates excellent rate capability, delivering 60 mAh g^{-1} reversible capacity at a current density of 1250 mA g^{-1}, which is ascribed to both fast Li transport kinetics in aqueous electrolytes and a sufficiently large interlayer distance of the host material modified by water. Our work reveals the complex nature of intercalation reactions in aqueous batteries, in which the reactivity of hydrated cations with the layered chalcogenide may lead to intriguing electrochemical and structural properties.

ASSOCIATED CONTENT

Supporting Information: Experimental and computational methods, additional electrochemical cycling data, *operando* XRD contour plots.

AUTHOR INFORMATION

Corresponding Author:

Leiting Zhang, *Department of Chemistry – Ångström Laboratory, Uppsala University, P.O. Box 538, 751 21 Uppsala, Sweden;* https://orcid.org/0000-0003-4057-7106; Email: leiting.zhang@kemi.uu.se

Authors:

Franziska Kühling, *Department of Chemistry – Ångström Laboratory, Uppsala University, Box 538, SE 751 21 Uppsala, Sweden;* https://orcid.org/0000-0001-7522-2845.

Agnes-Matilda Mattsson, *Department of Chemistry – Ångström Laboratory, Uppsala University, Box 538, SE 751 21 Uppsala, Sweden;* https://orcid.org/0000-0003-4399-2372.

Xu Hou, *Department of Chemistry – Ångström Laboratory, Uppsala University, Box 538, SE 751 21 Uppsala, Sweden;* https://orcid.org/0000-0003-0398-2006.

Gustav Ek, *Department of Chemistry – Ångström Laboratory, Uppsala University, Box 538, SE 751 21 Uppsala, Sweden;* https://orcid.org/0000-0003-4831-3842.

Thomas Dufils, *Department of Chemistry – Ångström Laboratory, Uppsala University, Box 538, SE 751 21 Uppsala, Sweden*.

Chao Zhang, *Department of Chemistry – Ångström Laboratory, Uppsala University, Box 538, SE 751 21 Uppsala, Sweden;* https://orcid.org/0000-0002-7167-0840.

William R. Brant, *Department of Chemistry – Ångström Laboratory, Uppsala University, Box 538, SE 751 21 Uppsala, Sweden;* https://orcid.org/0000-0002-8658-8938.

Kristina Edström, *Department of Chemistry – Ångström Laboratory, Uppsala University, Box 538, SE 751 21 Uppsala, Sweden*.

Erik J. Berg, *Department of Chemistry – Ångström Laboratory, Uppsala University, Box 538, SE 751 21 Uppsala, Sweden;* https://orcid.org/0000-0001-5653-0383.

Twitter handles:

@LeitingZhang, @chem_angstrom, @willrbrant1, @KristinaEdstrm2

Notes:

The authors declare no competing financial interest.

ACKNOWLEDGMENT

The authors acknowledge the Swedish Energy Agency (Grant 50119-1), Knut and Alice Wallenberg (KAW) Foundation (Grant 2017.0204), Swedish Research Council (2016-04069, 2022-03856), and Stiftelsen för Strategisk Forskning (SSF, FFL18-0269) for financial support and StandUp for Energy for base funding. F. K. acknowledges the Erasmus+ Programme for sponsoring her exchange study at Uppsala University.

REFERENCES

(1) Chao, D.; Zhou, W.; Xie, F.; Ye, C.; Li, H.; Jaroniec, M.; Qiao, S. Z. Roadmap for Advanced Aqueous Batteries: From Design of Materials to Applications. *Sci. Adv.* **2020**, *6* (21), eaba4098.

(2) Sui, Y.; Ji, X. Anticatalytic Strategies to Suppress Water Electrolysis in Aqueous Batteries. *Chem. Rev.* **2021**, *121* (11), 6654–6695.

(3) Suo, L.; Borodin, O.; Gao, T.; Olguin, M.; Ho, J.; Fan, X.; Luo, C.; Wang, C.; Xu, K. "Water-in-Salt" Electrolyte Enables High-Voltage Aqueous Lithium-Ion Chemistries. *Science* **2015**, *350* (6263), 938–943.

(4) Yamada, Y.; Usui, K.; Sodeyama, K.; Ko, S.; Tateyama, Y.; Yamada, A. Hydrate-Melt Electrolytes for High-Energy-Density Aqueous Batteries. *Nat. Energy* **2016**, *1* (10), 16129.

(5) Xie, J.; Liang, Z.; Lu, Y. C. Molecular Crowding Electrolytes for High-Voltage Aqueous Batteries. *Nat. Mater.* **2020**, *19* (9), 1006–1011.

(6) Yue, J.; Zhang, J.; Tong, Y.; Chen, M.; Liu, L.; Jiang, L.; Lv, T.; Hu, Y. sheng; Li, H.; Huang, X.; Gu, L.; Feng, G.; Xu, K.; Suo, L.; Chen, L. Aqueous Interphase Formed by CO_2 Brings Electrolytes Back to Salt-in-Water Regime. *Nat. Chem.* **2021**, *13* (11), 1061–1069.

(7) Zhao, J.; Zhang, J.; Yang, W.; Chen, B.; Zhao, Z.; Qiu, H.; Dong, S.; Zhou, X.; Cui, G.; Chen, L. "Water-in-Deep Eutectic Solvent" Electrolytes Enable Zinc Metal Anodes for Rechargeable Aqueous Batteries. *Nano Energy* **2019**, *57*, 625–634.

(8) Suo, L.; Borodin, O.; Sun, W.; Fan, X.; Yang, C.; Wang, F.; Gao, T.; Ma, Z.; Schroeder, M.; von Cresce, A.; Russell, S. M.; Armand, M.; Angell, A.; Xu, K.; Wang, C. Advanced

High-Voltage Aqueous Lithium-Ion Battery Enabled by "Water-in-Bisalt" Electrolyte. *Angew. Chemie - Int. Ed.* **2016**, *55* (25), 7136–7141.

(9) Zhang, H.; Xu, D.; Yang, F.; Xie, J.; Liu, Q.; Liu, D. J.; Zhang, M.; Lu, X.; Meng, Y. S. A High-Capacity Sn Metal Anode for Aqueous Acidic Batteries. *Joule* **2023**, *7* (5), 971–985.

(10) Chen, L.; Zhang, J.; Li, Q.; Vatamanu, J.; Ji, X.; Pollard, T. P.; Cui, C.; Hou, S.; Chen, J.; Yang, C.; Ma, L.; Ding, M. S.; Garaga, M.; Greenbaum, S.; Lee, H.-S.; Borodin, O.; Xu, K.; Wang, C. A 63 m Superconcentrated Aqueous Electrolyte for High-Energy Li-Ion Batteries. *ACS Energy Lett.* **2020**, *5* (3), 968–974.

(11) Jaumaux, P.; Yang, X.; Zhang, B.; Safaei, J.; Tang, X.; Zhou, D.; Wang, C.; Wang, G. Localized Water-In-Salt Electrolyte for Aqueous Lithium-Ion Batteries. *Angew. Chemie - Int. Ed.* **2021**, *60* (36), 19965–19973.

(12) Zhang, L.; Hou, X.; Edström, K.; Berg, E. J.; Zhang, L.; Hou, X.; Edström, K.; Berg, E. J. Reactivity of TiS_2 Anode towards Electrolytes in Aqueous Li-Ion Batteries. *Batter. Supercaps* **2022**, *5* (12), e202200336.

(13) Kovalenko, K. A.; Potapov, A. S.; Fedin, V. P.; Kolesnichenko, N. V; Ezhova, N. N.; Snatenkova, Y. M.; Yang, Y.; Jiang, H.; Xu, D. *Operando* Synchrotron X-Ray Diffraction Studies on TiS_2: The Effect of Propylene Carbonate on Reduction Mechanism. *J. Electrochem. Soc.* **2021**, *168* (3), 030514.

(14) Alvarez Ferrero, G.; Åvall, G.; Mazzio, K. A.; Son, Y.; Janßen, K.; Risse, S.; Adelhelm, P. Co-Intercalation Batteries (CoIBs): Role of TiS_2 as Electrode for Storing Solvated Na Ions. *Adv. Energy Mater.* **2022**, *12* (47), 2202377.

(15) Park, J.; Kim, S. J.; Lim, K.; Cho, J.; Kang, K. Reconfiguring Sodium Intercalation Process of TiS_2 Electrode for Sodium-Ion Batteries by a Partial Solvent Cointercalation. *ACS Energy Lett.* **2022**, *7* (10), 3718–3726.

(16) Whittingham, M. S. The Hydrated Intercalation Complexes of the Layered Disulfides. *Mater. Res. Bull.* **1974**, *9* (12), 1681–1689.

(17) Lerf, A.; SCHÖLLHORN, R. Solvation Reactions of Layered Ternary Sulfides A_xTiS_2, A_xNbS_2, and A_xTaS_2. *Inorg. Chem.* **1977**, *16* (11), 2950–2956.

(18) Schöllhorn, R.; Meyer, H. Cathodic Reduction of Layered Transition Metal Chalcogenides. *Mater. Res. Bull.* **1974**, *9* (9), 1237–1245.

(19) Mondal, A.; Vomiero, A. 2D Transition Metal Dichalcogenides-Based Electrocatalysts for Hydrogen Evolution Reaction. *Adv. Funct. Mater.* **2022**, *32* (52), 2208994.

(20) Mizushima, K.; Jones, P. C.; Wiseman, P. J.; Goodenough, J. B. Li_xCoO_2 ($0<x<1$): A New Cathode Material for Batteries of High Energy Density. *Mater. Res. Bull.* **1980**, *15* (6), 783–789.

(21) Gustafsson, O.; Schökel, A.; Brant, W. R. Design and Operation of an *Operando* Synchrotron Diffraction Cell Enabling Fast Cycling of Battery Materials. *Batter. Supercaps* **2021**, *4* (10), 1599–1604.

(22) SCHÖLLHORN, R. Solvated Intercalation Compounds of Layered Chalcogenide and Oxide Bronzes. In *Intercalation Chemistry*; Academic Press, 1982; pp 315–360.

(23) Yan, M.; He, P.; Chen, Y.; Wang, S.; Wei, Q.; Zhao, K.; Xu, X.; An, Q.; Shuang, Y.; Shao, Y.; Mueller, K. T.; Mai, L.; Liu, J.; Yang, J.; Yan, M.; Wang, S.; Yang, J.; He, P.; Wei, Q.;

Zhao, K.; Xu, X.; An, Q.; Shuang, Y.; Mai, L.; Chen, Y.; Shao, Y.; Mueller, K. T.; Liu, J. Water-Lubricated Intercalation in $V_2O_5 \cdot nH_2O$ for High-Capacity and High-Rate Aqueous Rechargeable Zinc Batteries. *Adv. Mater.* **2018**, *30* (1), 1703725.

(24) Zhang, N.; Dong, Y.; Jia, M.; Bian, X.; Wang, Y.; Qiu, M.; Xu, J.; Liu, Y.; Jiao, L.; Cheng, F. Rechargeable Aqueous Zn-V_2O_5 Battery with High Energy Density and Long Cycle Life. *ACS Energy Lett.* **2018**, *3* (6), 1366–1372.

(25) Shin, J.; Shin Choi, D.; Jeong Lee, H.; Jung, Y.; Wook Choi, J.; Shin, J.; Lee, H. J.; Choi, J. W.; Choi, D. S.; Jung, Y. Hydrated Intercalation for High-Performance Aqueous Zinc Ion Batteries. *Adv. Energy Mater.* **2019**, *9* (14), 1900083.

(26) Xiao, B. Intercalated Water in Aqueous Batteries. *Carbon Energy* **2020**, *2* (2), 251–264.

(27) Fleischmann, S.; Shao, H.; Taberna, P. L.; Rozier, P.; Simon, P. Electrochemically Induced Deformation Determines the Rate of Lithium Intercalation in Bulk TiS_2. *ACS Energy Lett.* **2021**, *6* (12), 4173–4178.

(28) Rempe, S. B.; Pratt, L. R.; Hummer, G.; Kress, J. D.; Martin, R. L.; Redondo, A. The Hydration Number of Li^+ in Liquid Water. *J. Am. Chem. Soc.* **2000**, *122* (5), 966–967.

(29) Zhi, J.; Zehtab Yazdi, A.; Valappil, G.; Haime, J.; Chen, P. Artificial Solid Electrolyte Interphase for Aqueous Lithium Energy Storage Systems. *Sci. Adv.* **2017**, *3* (9), e1701010.

(30) Droguet, L.; Hobold, G. M.; Lagadec, M. F.; Guo, R.; Lethien, C.; Hallot, M.; Fontaine, O.; Tarascon, J. M.; Gallant, B. M.; Grimaud, A. Can an Inorganic Coating Serve as Stable SEI for Aqueous Superconcentrated Electrolytes? *ACS Energy Lett.* **2021**, *6*, 2575–2583.

(31) Mähler, J.; Persson, I. A Study of the Hydration of the Alkali Metal Ions in Aqueous

Solution. *Inorg. Chem.* **2012**, *51* (1), 425–438.

(32) Tang, W.; Song, X.; Du, Y.; Peng, C.; Lin, M.; Xi, S.; Tian, B.; Zheng, J.; Wu, Y.; Pan, F.; Loh, K. P. High-Performance $NaFePO_4$ Formed by Aqueous Ion-Exchange and Its Mechanism for Advanced Sodium Ion Batteries. *J. Mater. Chem. A* **2016**, *4* (13), 4882–4892.